10594 *Macromolecules* **2010**, *43*, 10594–10599
DOI: 10.1021/ma1016117

Macromolecules
ARTICLE

Translocation Dynamics of Poly(styrenesulfonic acid) through an α-Hemolysin Protein Nanopore

Qianjin Chen,*,† Jin Liu,‡ Anna E. P. Schibel,‡ Henry S. White,*,‡ and Chi Wu*,†

†*Department of Chemistry, The Chinese University of Hong Kong, Shatin, N. T., Hong Kong, and*
‡*Department of Chemistry, University of Utah, 315 S.1400 E, Salt Lake City, Utah 84112, United States*

Received July 20, 2010; Revised Manuscript Received October 29, 2010

ABSTRACT: The transport of linear anionic poly(styrenesulfonic acid) (PSS) chains through an α-hemolysin protein channel, embedded in a lipid bilayer which is suspended on a glass nanopore membrane, is reported as a function of applied voltage and chain length. By investigating individual event details, we observed mainly four types of events with distinct bilevel current blockades. The majority of the translocation events have a shallow block level with current decrease of ∼60%, followed by a deep block level with current decrease of ∼85%. A mechanism for PSS translocation is proposed and compared with that for ssDNA translocation through the ion channel. Although similar bilevel blockades are observed for both PSS and ssDNA, differences in the chain rigidity between PSS and ssDNA result in distinct populations for each type of event and quite different characteristic translocation times. At a voltage of 160 mV, the PSS chains are more likely to thread the narrowest constriction and translocate through the pore than to escape from the vestibule against the applied voltage gradient. Increasing the applied voltage decreases the duration time of chain translocation through the pore, while increasing the characteristic time of the PSS within the vestibule. We further find that the translocation event rate is exponentially dependent on the applied potential while the most likely duration time also decreases exponentially with the voltage. These results demonstrate how the nature of the polyelectrolyte chain influences translocation process through protein ion channels.

Introduction

Ever since the first observation of the single-stranded DNA (ssDNA) passage through an α-hemolysin (αHL) pore embedded in a planar lipid bilayer,[1] synthetic and biological nanopores have been increasingly used to investigate biopolymer translocation mechanisms.[2−25] The protein ion channel is embedded within a lipid bilayer, and an electric potential is applied across the membrane. Driven by the electric force, a biopolymer molecule can pass through the nanopore, resulting in a transient current decrease related to the pore geometry and chain nature such as monomer size, length, rigidity, and conformation.[26] This sensing method is of great scientific interest because it provides a unique view of polymer dynamics and structure at the single-molecule level, and it may serve as a useful model system in the development of our understanding of biologically relevant nanoscale physical and chemical processes.[27−29] So far, wild-type (WT) and engineered αHL have been used to develop methods to sequence DNA,[2−8] to understand the dynamics of confined neutral polymers,[9−11] and charged polyelectrolytes,[12−14] and to measure the kinetics of DNA duplex and hairpin unzipping,[15−17] and DNA−protein interaction.[18] It was even used as a nanoreactor to monitor the individual covalent reaction of single polymer chains.[19,20] The αHL pore consists of a vestibule on the cis side and a transmembrane β-barrel on the trans side with a pore length around 10 nm. The opening of the vestibule at the cis side is around 2.9 nm, and the diameter of the vestibule's cavity is around 4.1 nm. The average internal diameter of the β-barrel is around 2 nm. These two pore domains are separated by a constriction of 1.4 nm diameter.[30,31]

There are several recent systematic studies of the mechanistic details of DNA translocation through the αHL pore.[3,28,31] Three current levels were found for ssDNA translocation: the open state, a mid-amplitude state, and a low-amplitude state.[3,28] The low-amplitude state (∼0−30% of the open state) is generally associated with translocation of a polynucleotide molecule through the pore.[2,3,24,28] The mid-amplitude (∼30−85% of the open state) is believed to correspond to the polynucleotide molecule residing in the vestibule position of the pore.[3,28] These results are also confirmed by molecular dynamic simulation.[31] Similar multilevel current states for double-stranded (dsDNA) within a solid-state nanopore with diameter around 10 nm are also reported.[25,26] The complex features of events are attributed to folded chain configurations in the nanopore. It was these works that inspired us to study how the nature of the polymer chain affects the translocation dynamics through the nanopore. More important, we like to check whether there are two chain conformation populations (coiled and collapsed) during the coil-to-globule transition so that we might be able to tell whether such a transition is the first-order or the second-order one. In this study, we start with a long and much more flexible synthetic homopolyelectrolyte chain, driven through αHL, in order to provide further insight into polymer translocation mechanisms. Recently, Murphy et al.[14] measured the current signatures of sodium poly(styrenesulfonate) applied with electric force with the protein channel. They found that the average translocation time was proportional to the molecular weight and inversely proportional to the applied voltage. But the duration time distribution was significantly different from those for DNA and RNA. However, detailed information about individual events was not presented and systematically analyzed.

We recently developed a process for the fabrication of glass membranes containing a single conical shaped pore of radii from 10 nm to several micrometers[32,33] and for the first time applied the glass nanopore membrane (GNM) for ion channel recordings.[34]

*To whom correspondence should be addressed.

 Published on Web 12/03/2010

The advantages for the single ion channel recording using the GNM lie in, first, insertion and removal of αHL protein can easily be achieved by controlling the pressure inside the capillary, which influences the bilayer structure suspended across the pore orifice, and, second, because of the smaller size of GNM compared with a pore of ~50 μm in a polymer membrane (which is normally used for single ion channel recording), there is large reduction of bilayer area, resulting in lower noise in ion channel recordings. In this work, using WT-αHL protein and GNM supports, we investigated the translocation of individual synthetic flexible PSS chains through the ion channel in a 1.0 M KCl/25 mM tris buffer solution. Our results show that there are two distinct types of current blockades for the events with three current levels, a similar result observed for ssDNA.[3,35] However, a PSS chain behaves more flexible in the vestibule at the cis side and takes longer time to translocate through the nanopore for each monomer than a ssDNA chain. The dynamics of the flexible polyelectrolyte translocation events are also analyzed in this study.

Experimental Section

A single GNM with 1430 nm radius was used throughout this study. The fabrication details have been previously discribed.[32,33] The GNM was pretreated by soaking the entire glass capillary (inside and outside) in a 0.1 M HNO_3 solution for 10 min. Then the glass capillary was rinsed with copious amounts of ultrapure H_2O, EtOH, and HPLC CH_3CN before being filled and fully immersed in a 2% v/v solution of 3-cyanopropyldimethlychlorosilane (Gelest Inc.) in CH_3CN for 12 h. Deposition of the −CN-terminated silane monolayer on the exterior surface of the GNM results in lipid monolayer formation on the glass surface and a suspened lipid bilayer across the nanopore orifice.[34] The capillary was then rinsed sequentially with CH_3CN, EtOH, and H_2O. The modified GNM after silanization can be stored indefinitely in EtOH ready prior to use in ion channel recordings.

1,2-Diphytanoyl-*sn*-glycero-3-phosphocholine (DPhPC) (Avanti Polar Lipids, Alabster, AL) and WT-αHL toxin from *Staphylococcus aureus* (Sigma) were used throughout the experiments. The lipid solution is prepared in following way: 1 mL of a 10 mg/mL DPhPC solution in chloroform was first dried under high purity N_2. After drying, the solid lipids were dissolved in decane at 10 mg/mL and stored at −25 °C before using. The stock solution for WT-αHL protein was prepared by dissolving 0.5 mg of WT-αHL protein in 0.5 mL of ultrapure H_2O, and after fully dissolved, the solution was separated into the 20 μL plastic tubes. Each tube containing protein solution was diluted to 1.5 mL with the buffer solution and then stored at 5 °C ready for use. The poly(styrenesulfonic acid) (PSS) samples with hydrodynamic sizes much larger than the ion channel pore were purchased from Polymer Source with weight-averaged molecular M_w = 27 300, 136 500, and 2 700 000 g/mol with polydispersity indices of 1.03, 1.05, and 1.12, respectively. The PSS samples were used without any further purification. PSS sample stock solutions were prepared using 1.0 M KCl/25 mM tris buffer solution (pH = 7.35). The molar concentration of the stock solution for the 27 300 and 136 500 g/mol samples was ~20 μM, while that for the 2 700 000 g/mol sample was 1 μM, which are all lower than their respective overlap concentrations (c^*). Each stock solution was kept at 5 °C for at least 1 week before use to ensure that the polyelectrolyte was fully dissolved.

Prior to bilayer formation, the GNM was inserted into a pipet holder (Dagan), and the end of the glass capillary containing the membrane and nanopore was soaked in the electrolyte solution. After the formation of a lipid bilayer across the nanopore in the GNM,[33] the αHL protein solution was added to the solution with a final protein concentration of ~40 nM. After reconstitution of an operative αHL channel with proper conductance, the stock PSS solution was added into the buffer solution with a final polymer molar concentration suitable for recording individual PSS translocation events. Data were collected at least 10 min after addition of the PSS so that the polymer was uniformly dispersed.

The ion channel instrumentation was interfaced to Dell PC computer through a National Instrument (NI) PCI-6251 data acquisition board via a BNC-2090 (NI). A Dagan Chem-Clamp voltammeter/amperometer was used as a potentiostat. Current−time ($i-t$) curves were recorded using in-house virtual instrumentation written in NI Labview 8.5. The ionic current was monitored at a 100 kHz sampling rate with a 10 kHz filter. All experiments were carried out inside a home-built Faraday cage at room temperature (24 ± 1 °C). Analysis of current blockade amplitudes and event durations was performed using Igor Pro 6.02 and QuB software package. Events with duration time less than 100 μs are discarded and not analyzed because the 10 kHz filter artificially biases these events. Between 500 and 3000 events were recorded for each experiment.

Results and Discussion

In the absence of PSS samples, the conductance of αHL pore in 1.0 M KCl/25 mM tris buffer was 0.98 ± 0.03 and 1.03 ± 0.02 nS at 80 and 140 mV, respectively, in good agreement with literature values.[3,12,16,34] The addition of PSS in the buffer solution to the cis side of αHL resulted in current blockade events in the current trace. Figure 1 shows part of a current trace recorded for PSS 27 300 and 136 500 g/mol at both 80 and 140 mV. The background current traces are also presented for comparison (Figure 1A,D). No current blockades were observed in the background experiments. We notice that for voltage of 80 mV there are few events at a current level of 34−50 pA (Figure 1B,C), and for voltage of 140 mV, besides the shallow events at 42−62 pA, there are also many deep events at 5−25 pA (Figure 1E,F). Close inspection shows that for the deep events there is normally a preshallow level followed by a deep level. This interesting phenomenon was observed in the experiments of all the three molecular weight chains, with all types of events shown in Figure 2. The event current levels I_O, I_S, and I_D, and the duration time, t_d, are also defined in Figure 2.

For type A events, there is only a single deep current level (I_D) at ~15% of the open-channel current (I_O). We believe that this is the direct translocation of a PSS chain through the β-barrel, exiting on the trans side of the pore. For type B events, there is only a single shallow current level (I_S) at 30−45% of the open-channel current. We assume that this is the entry of PSS chain into the vestibule and exit from the cis side, without threading through the narrowest constriction of the pore. For type C events, there are two blockade states: a shallow level followed by a deep stage within the same event. The deep level has a similar current amplitude as type A. This event is considered to correspond to the situation that the PSS chain is captured in the vestibule before it translocates through the β-barrel to exit at the trans side. For type D events, there is a shallow block, followed by a short deep block and a second shallow block within the same event. This event is presumed to correspond to a PSS chain that explores the vestibule, threads into the β-barrel partially, but retracts back into the vestibule and eventually exits the pore from the cis side. For type E and F events, there are multiple shallow segments separated by a deep segment. It is presumed that the PSS chain is trapped in the vestibule, and then it threads into part of the β-barrel and retracts back into the vestibule. This threading and retracting process might repeat for many times before the chain finally exits from the cis side of the pore (for type E events) or translocates through the β-barrel to exit at the trans side (for type F events). We only observed a few type E or F events in thousands of total events. In all types of events, PSS is captured by the pore, but only in types A, C, and F does PSS translocation occur, from cis to trans side. For translocation events of types C and F, only the last deep segment is considered as translocation. The types of

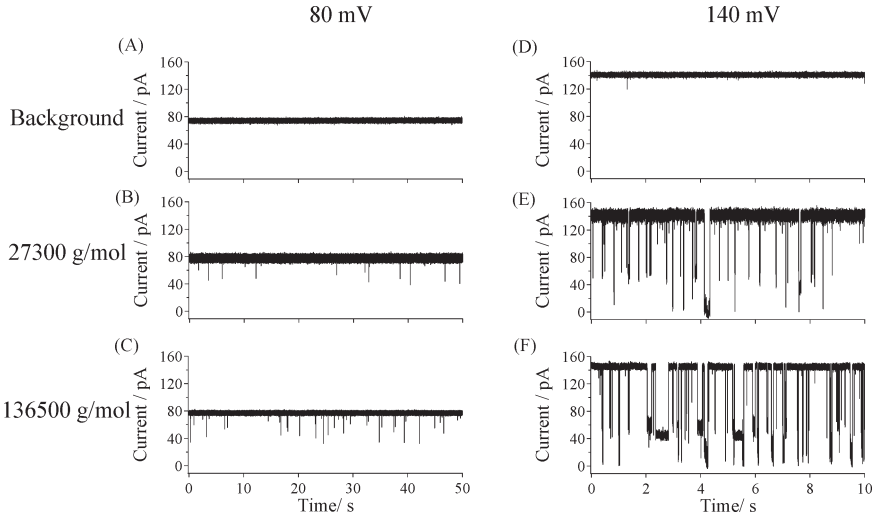

Figure 1. Measured ionic current versus time for PSS in 1.0 M KCl/25 mM tris buffer, pH = 7.35: (A, D) open channel background at 80 and 140 mV; (B, E) current trace at for PSS 27 300 g/mol (1.1 μM) at 80 and 140 mV, respectively; (C, F) current trace for PSS 136 500 g/mol (2.0 μM) at 80 and 140 mV, respectively.

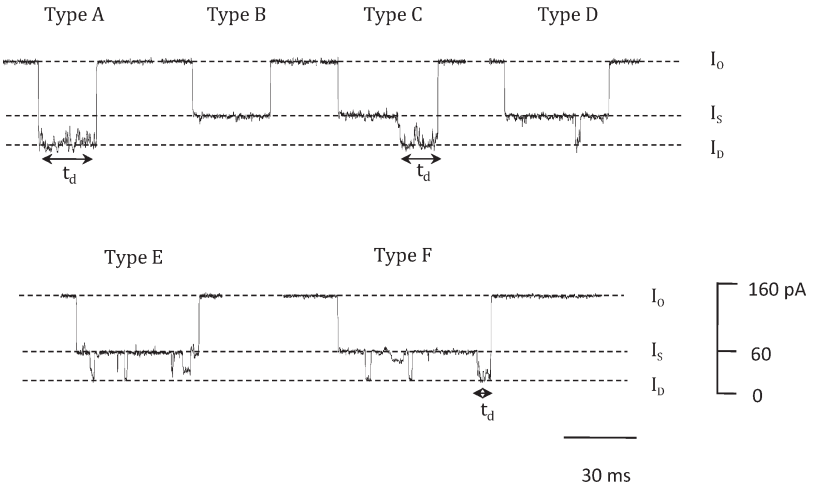

Figure 2. Interactions of PSS 136 500 g/mol with αHL pore at 140 mV with six types of events. Three current levels of I_O, I_S, and I_D and duration time (t_d) are defined as illustrated. Current and time scale bars are also provided.

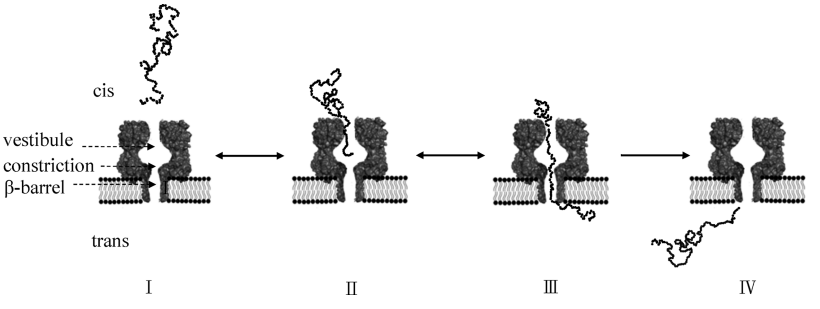

Figure 3. Model of the interaction of a PSS chain with αHL pore. The concept and figure are adapted from ref 3.

events are consistent with the description of ssDNA translocation through αHL in the literature.[3,35]

A scheme for PSS capture and translocation within the nanopore, adapted from ref 3, is depicted in Figure 3 to interpret the various event types. Before a typical translocation event, a PSS chain collides with the mouth of the pore and occupies the vestibule region of the pore (II), leading to a current state at a shallow level. The type B event results when the chain retracts back into the cis compartment (II−I). Alternatively, one end of the polymer may thread through the narrow constriction and transport into the β-barrel by electrophoresis. Electroosmotic solvent flowing through the channel happens in the same direction (cis to trans) and can further assist PSS transport. At this point, the chain is more likely to continue to thread through β-barrel and exit from the trans side of the pore (III−IV). The effect of the applied field on the PSS chain during this process is strongest.[3,36] The translocation process (III) was observed experimentally by the abrupt reduction of current by 85% of the open channel current level (types A, C, and F). The type of straightforward PSS translocation events (type A), however, only

comprises 11.7% of the total translocation events (types A, C, and F) at 140 mV (see Table 1). The majority are type C events with a shallow current followed by a deep current level within the event. For a chain already threading into the β-barrel, instead of going further with a successful translocation, it is also possible to retract back into the vestibule and exit the pore from the same side (III−II−I), leading to type D events. With very low possibility, the threading and retracting action may repeat several times within one event before the chain finally exits or passes through the pore, resulting in type E or F events, respectively. The confinement of chain or segment in a nanoscopic tube has been extensively studied both theoretically and experimentally.[37−39]

The scatter plot of type B events for PSS 136 500 g/mol at 140 mV is shown in Figure 4A, where each point represents a single event. The preshallow segment of type C events is extracted and defined as type C shallow events, while the remaining deep segment is defined as type C deep events. Figure 4B shows the scatter plot of type C shallow events and type A, C, and F deep events. We can easily tell the boundary for shallow and deep current level is around 30%, with an average deep current level of 15%. Closer inspection also shows there are two different situations for the type B events. One is located at a current level of 42 ± 3% of the open current, and the other is at 31 ± 1%. But for type C shallow events (red color in Figure 4B), it appears that there is only one current population at 42 ± 3% of the open current. We infer that for the current level at 42 ± 3% the end of the chain takes an extended conformation in the vestibule, and for the current level at 31 ± 1%, it may fold itself, resulting in larger current blockade. Chains with folded conformation are less likely to translocate through the pore. Hence, there is no obvious events population at 31 ± 1% for type C shallow events, as shown in Figure 4B.

Duration time distributions for translocation events (types A, C, and F) are very broad, ranging from 0.1 to 2000 ms. We infer from this result that various chain conformation exist in the solution, although the polydispersity of synthetic polymer contributes as well to the distribution. For a voltage of 140 mV, roughly 94.4% of all events are located in the range of 0−200 ms, shown in Figure 5A with a bin size of 14 ms. The histogram exhibits a clear peak, defined as t_p, the most likely duration time. For a voltage of 120 mV, roughly 93.5% of the events are located in the same range, as shown in the histogram in Figure 5B, with the same bin size. We found that the most likely duration time increased from 20 to 27 ms, as the voltage decreased from 140 to 120 mV. The characteristic duration time for each monomer of PSS at 120 mV is ~36.6 μs, much longer than that of adenine for $(dA)_{100}$, 19.2 μs, and cytosine for $(dC)_{100}$, 7.6 μs, in 1.0 M KCl/10 mM tris, pH 8.5 at 25 °C,[7] although the molecular size of styrenesulfonic acid is smaller than nucleotide. The possible reasons for this will be explained later. For type B events, the time distribution displays an exponential decay, with a time constant τ, as shown in Figures 5C and 5D at 140 and 120 mV, respectively. The bin time increment used in the figures is 1 ms. When we decreased the applied voltage, the duration time shifts to a shorter time, with the decay time constant decreasing from 5.52 to 3.34 ms. We can interpret this change as reflecting the dynamics of chain in the vestibule. When the applied voltage is higher, the captured PSS is subjected to a stronger electric force, and hence more time is required to exit the pore from cis side by thermal motion.

The percentage for each type of events for various potentials is listed in Table 1. The percentage of types E and F are very small (< 0.1%); hence, they are not presented. For a voltage of 140 mV, type A 5.4%, type B 52.9%, type C 40.6%, and type D 1.0%. At this voltage, the chance for a PSS chain captured in the vestibule

Table 1. Distribution of Types of PSS Events (percent) at Various Voltages[a]

voltage (mV)	type A (%)	type B (%)	type C (%)	type D (%)	type A/(type A + C) (%)
110	2.2	93.5	3.2	1.0	40.3
120	3.0	84.9	10.8	1.3	21.6
130	4.9	72.9	20.4	1.7	19.4
140	5.4	52.9	40.6	1.0	11.7
150	5.8	38.7	54.4	1.0	9.6
160	3.4	27.0	69.0	0.5	4.8

[a] The last column represents percentage of direct translocation events (no shallow preblockade) of total number of translocation events. Since the population of type E and F events are really small, their percentages are not listed here.

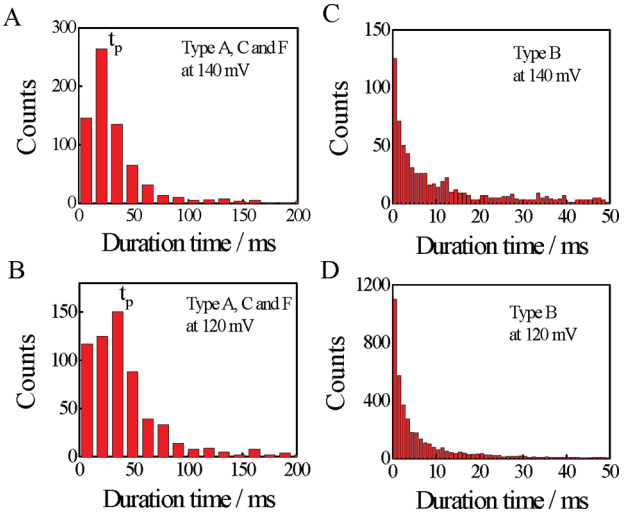

Figure 5. Histogram of duration time for translocation events (types A, C, and F) at 140 mV (A) and 120 mV (B) and events for vestibule configuration (type B) at 140 mV (C) and 120 mV (D) for PSS 136 500 g/mol (2.0 μM) in 1.0 M KCl/25 mM tris buffer, pH = 7.35.

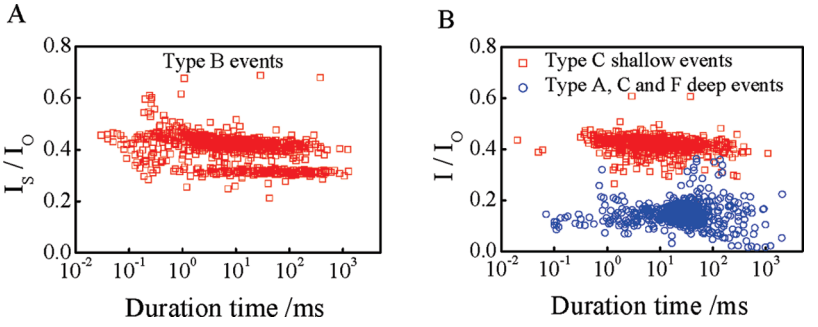

Figure 4. (A) Scatter plot for different type B events for PSS 136 500 g/mol (2.0 μM) in 1.0 M KCl/25 mM tris buffer, pH = 7.35, at 140 mV. Two different current block levels are found. (B) Scatter plot for preshallow segment of type C events (in red) and the deep segment for translocation events (types A, C, and F) (in blue).

that also exits from the cis side (52.9%) is roughly the same as that of a PSS chain threading the narrowest constriction and then translocate the β-barrel (40.6%). Notice that as the voltage increased, the percentage of type B events decreased dramatically from 93.5% at 110 mV to 27.0% at 160 mV, indicating that a chain captured in the vestibule is more likely to translocate through the β-barrel and exit from the trans side, rather than escaping from cis side without threading through the narrowest constriction. In addition, it is found that the percentage of direct translocation events, i.e., those that do not show shallow pre-blockades, [type A/(type A + type C)] decreases as the potential increases. To compare our results with ssDNA events using WT-αHL at 120 mV, the percentages for individual type events at 120 mV are: type A 67.6%, type B 19.6%, type C 10.2%, type D 0.6% for 92-mer ssDNA;[3] type A 3.0%, type B 84.9%, type C 10.8%, type D 1.3% for PSS 136 500 g/mol (740 repeat units). We find that the percentage of translocation events (types A and C) of the total events for PSS is much less than that of ssDNA and the percentage of direct translocation events ([type A/(type A + type C)] = 21.6%) is also less than ssDNA (86.9%). In other words, for the same voltage applied, a chain captured in the vestibule is less likely to thread the narrowest constriction for PSS than ssDNA, and for chains that do translocate the nanopore, PSS is more likely to be captured in the vestibule before threading into the narrowest constriction than ssDNA. We interpret these differences in terms of the nature of polyelectrolyte chain. In an aqueous solution containing electrolyte, flexible polyelectrolyte chains becomes crumpled and coiled, surrounded by a diffused layer of counterions. A fraction of the counterions, together with the negative charges along the polymer chain, constitute many dipoles under the influence of an applied electric field. Because ssDNA chains are less coiled and much more extended than PSS chains, although each PSS chain possesses more ionogenic sites than an ssDNA chain per unit mass, the alignment of dipoles on a PSS chain along the electric field direction is less ordered than that on an ssDNA chain. The effective electric field force is proportional to both the total projected dipole moment along the electric field and the gradient of the electric field near the protein channel. Therefore, the PSS coiled chain with less aligned dipoles along its backbone is subjected to a weaker force than the ssDNA extended chain under the same electric field gradient. On the other hand, a coiled chain has to be stretched into a string of small "blobs" with diameters less than the pore size before it can translocate, which means that an additional entropy barrier has to be overcome for a coiled chain. This might explain why a longer characteristic duration time is required for the PSS translocation; namely, the coiled PSS chain requires a longer time to adjust itself and be stretched in the vestibule before threading into the 1.4 nm constriction between vestibule and β-barrel.

The detailed process of polyelectrolyte translocation through a narrow pore remains poorly understood, but there are several theories describing the possible phenomena.[12] The voltage dependence of translocation event frequency (f) is generally described by a Van't Hoff−Arrhenius law: $f = f_0 \exp(|V|/V_0)$ with $f_0 = \kappa\nu \exp(-U^*/kT)$, depending on the activation energy U^* (κ and ν are the probability factor and the frequency factor, respectively),[40] and $|V|/V_0 = ze|V|/kT$, a barrier reduction factor due to the applied voltage, with z, the magnitude of the effective total number of elementary charges (e) on the polymer.[41] This effective charge is related to several effects: access resistance, charge distribution, and the conformation of the polyelectrolyte at the pore entrance.[12,42] The data from 80 to 160 mV are described by the function with $f_0 = 1.05 \pm 0.68$ min^{-1} and $V_0 = 29.3 \pm 3.4$ mV. The deduced effective charge of the polyelectrolyte is $z = 0.88$. Since the effect of the applied field on the polyelectrolyte is strongest in the β-barrel, the value of z reflects the effective charge along the chain within the channel, indicating most of the charges on the polymer are effectively screened by counterions. To further estimate the activation energy (U),[12,40,41] the frequency factor ν is estimated by a barrier penetration calculation to be ~650 min^{-1} by $\nu \approx CDA/l$,[43] where C is the bulk concentration of the polymer, $C = 2.0$ μM, D is the polymer diffusion coefficient, $D \approx 3 \times 10^{-7}$ cm^2 s^{-1} for PSS 136500 g/mol in 1.0 M KCl tris buffer solution estimated by DLS measurement at room temperature, A is the cross-sectional area of the channel, $A \approx 3 \times 10^{-14}$ cm^2, and l is the width of the barrier, $l \approx 10^{-6}$ cm.[30] The resulting calculated activation energy is roughly 6 kT. These values of z and U are of the same order as other values for different polyelectrolyte at 1.0 M KCl electrolyte solution. For ssDNA,[40,42] $z = 1.9$ and $U \approx 8\,kT$, or for dextran sulfate,[12] $z = 0.95$ and $U \approx 10\,kT$. On the other hand, in the region below 100 mV, the probability of deep events is very low.

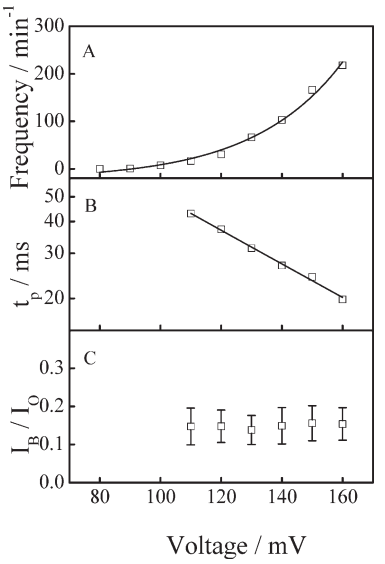

Figure 6. Voltage dependence of (A) translocation event frequency, where data are fitted with an exponential decay with $f_0 = 1.05 \pm 0.68$ min^{-1} and $V_0 = kT/ze = 29.3 \pm 3.4$ mV, (B) most probable duration time (t_p) for translocation, and (C) normalized ionic current $\langle I_B \rangle / \langle I_O \rangle$ for translocation events (types A and C) for PSS 136 500 g/mol in 1.0 M KCl/25 mM tris buffer, pH = 7.35.

In the curve shown in Figure 6A, there is a voltage threshold for translocation events. Note that for 80 mV there are very few translocation events, while for 100 mV the frequency starts to significantly increase with voltage. So, this should be the threshold to overcome the entropy necessary to confine the coiled chain inside the pore. We assume the threshold electric force to insert a chain into the protein channel is equal to the confinement force:[44] $zeV/L \approx k_BT/D_{pore}$, where L and D_{pore} are the length and diameter of the tube and V is the threshold voltage to drive a chain into the tube, leading to $z = 0.67$. The value from this simple model agrees well with the results from the voltage dependence of event frequency ($z = 0.88$).

The most likely translocation duration time t_p as a function of voltage applied was analyzed in Figure 6B. The dependence of duration time can be well fit by an exponential decay with $V_c = 65.4 \pm 19.1$ mV. The effective charge of the polyelectrolyte inside the pore z_{pore} is 0.39 ± 0.11.[12] The normalized ionic current for translocation events is constant, $\langle I_B \rangle / \langle I_O \rangle = 0.15 \pm 0.04$, in the range of applied voltage (Figure 6C). Since the diameter for single-stranded DNA chain is around 1.4 nm, almost the same size as the narrow constriction and slightly smaller than the β-barrel of the channel, the current level for DNA translocation $\langle I_B \rangle / \langle I_O \rangle$ is about 9% or 12%, depending on the orientation of DNA entering the pore.[45] Considering that the diameter for PSS

chain is much smaller (~0.3 nm for styrene monomer), the cross section available for ion motion inside the pore, hence, is larger, resulting a higher $\langle I_B \rangle / \langle I_O \rangle$ value for PSS.

Conclusion

We have observed the translocation events of individual PSS chains through the protein ion channel and presented an analysis for various types of current blockades. The current blockade for each event can be regarded as a sequence of shallow (~40% of open channel) and deep (~15% of open channel) conductance state. The shallow current level is attributed to a PSS chain captured in the vestibule of protein nanopore with two distinct configurations. The chain trapped in the vestibule can either escape from the cis side (type B events) or continue to thread into the β-barrel for a successful translocation, leading to a deep current block. We further find that the duration time for a PSS chain staying in the vestibule increases with increasing voltage while the possibility for its escaping from the vestibule to cis compartment decreases. By analyzing the nature of polyelectrolyte chains, e.g., flexibility, charge density, and activation energy for the translocation, we are able to explain translocation differences between PSS and ssDNA. We also find that a PSS chain takes a much longer time to translocate each monomer segment through the pore than an ssDNA chain, probably due to less effective electric force caused by less aligned dipoles along the PSS chain backbone as well as the additional entropy barrier for stretching the more coiled PSS chain. Our results may give new insight into the flexibility and charge density property of polyelectrolyte chains for its dynamics in a nanoscale volume.

Acknowledgment. This work was supported by the Defense Advanced Research Project Agency (FA9550-06-C-00C) and the National Science Foundation (CHE-0616505). In addition, the financial support of the National Natural Scientific Foundation of China (NNSFC) Projects (20934005 and 50773077) and the Hong Kong Special Administration Region Earmarked Project (CUHK4039/08P, 2160361 and CUHK4042/09P, 2160396) is gratefully acknowledged.

References and Notes

(1) Kasianowicz, J. J.; Brandin, E.; Branton, D.; Deamer, D. W. *Proc. Natl. Acad. Sci. U.S.A.* **1996**, *93*, 13770.
(2) Howorka, S.; Cheley, S.; Bayley, H. *Nature Biotechnol.* **2001**, *19*, 636.
(3) Maglia, G.; Restrepo, M. R.; Mikhailova, E.; Bayley, H. *Proc. Natl. Acad. Sci. U.S.A.* **2008**, *105*, 19720.
(4) Stoddart, D.; Heron, A. J.; Mikhailova, E.; Maglia, G.; Baley, H. *Proc. Natl. Acad. Sci. U.S.A.* **2009**, *106*, 7702.
(5) Clarke, J.; Wu, H. C.; Jayasinghe, L.; Patel, A.; Reid, S.; Bayley, H. *Nature Nanotechnol.* **2009**, *4*, 265.
(6) Astier, Y.; Braha, O.; Bayley, H. *J. Am. Chem. Soc.* **2006**, *128*, 1705.
(7) Meller, A.; Nivon, L.; Brandin, E.; Golovchenko, J.; Branton, D. *Proc. Natl. Acad. Sci. U.S.A.* **2000**, *97*, 1079.
(8) Ashkenasy, N.; Sanchez-Quesada, J.; Bayley, H.; Ghadiri, M. R. *Angew. Chem., Int. Ed.* **2005**, *44*, 1401.
(9) Krasilnikov, O. V.; Rodrigues, C. G.; Bezrukov, S. M. *Phys. Rev. Lett.* **2006**, *97*, 018301.
(10) Movileanu, L.; Cheley, S.; Bayley, H. *Biophys. J.* **2003**, *85*, 897.
(11) Bezrukov, S. M.; Vodyanoy, I.; Parsegian, V. A. *Nature* **1994**, *370*, 279.
(12) Brun, L.; Pastoriza-Gallego, M.; Oukhaled, G.; Mathe, J.; Bacri, L.; Auvray, L.; Pelta, J. *Phys. Rev. Lett.* **2008**, *100*, 158302.
(13) Gibrat, G.; Pastoriza-Gallego, M.; Thiebot, B.; Breton, M.; Auvray, L.; Pelta, J. *J. Phys. Chem. B* **2008**, *112*, 14687.
(14) Murphy, R. J.; Muthukumar, M. *J. Chem. Phys.* **2007**, *126*, 051101.
(15) Sauer-Budge, A. F.; Nyamwanda, J. A.; Lubensky, D. K.; Branton, D. *Phys. Rev. Lett.* **2003**, *90*, 238101.
(16) Tropini, C.; Marziali, A. *Biophys. J.* **2007**, *92*, 1632.
(17) Mathe, J.; Visram, H.; Viasnoff, V.; Rabin, Y.; Meller, A. *Biophys. J.* **2004**, *87*, 3205.
(18) Hornblower, B.; Coombs, A.; Whitaker, R. D.; Kolomeisky, A.; Picone, S. J.; Meller, A.; Akeson, M. *Nature Methods* **2007**, *4*, 315.
(19) Shin, S.; Bayley, H. *J. Am. Chem. Soc.* **2005**, *127*, 10462.
(20) Bayley, H.; Luchian, T.; Shin, S.-H.; Steffensen, M. In *Single Molecules and Nanotechnology*; Rigler, R., Vogel, H., Eds.; Springer: Heidelberg, 2008.
(21) Kasianowicz, J. J.; Robertson, J. W. F.; Chan, E. R.; Reiner, J. E.; Stanford, V. M. *Annu. Rev. Anal. Chem.* **2008**, *1*, 737.
(22) Dorp, S. V.; Keyser, U. F.; Dekker, N. H.; Dekker, C.; Lemay, S. G. *Nature Phys.* **2009**, *5*, 347.
(23) Smeets, R. M. M.; Keyser, U. F.; Krapf, D.; Wu, M.; Dekker, N. H.; Dekker, C. *Nano Lett.* **2006**, *6*, 89.
(24) Meller, A.; Nivon, L.; Branton, D. *Phys. Rev. Lett.* **2001**, *86*, 3435.
(25) Li, J.; Gershow, M.; Stein, D.; Brandin, E.; Golovchenko, J. A. *Nature Mater.* **2003**, *2*, 611.
(26) Storm, A. J.; Chen, J. H.; Zandbergen, H. W.; Dekker, C. *Phys. Rev. E* **2005**, *71*, 051903.
(27) Henriquez, R. R.; Ito, T.; Sun, L.; Crooks, R. M. *Analyst* **2004**, *129*, 478.
(28) Butler, T. Z.; Gundlach, J. H.; Troll, M. A. *Biophys. J* **2006**, *90*, 190.
(29) Howorka, S.; Siwy, Z. *Chem. Soc. Rev.* **2009**, *38*, 2360.
(30) Song, H.; Hobaugh, M. R.; Shustak, C.; Cheley, S.; Bayley, H.; Gouaux, J. E. *Science* **1996**, *274*, 1859.
(31) Muthukumar, M.; Kong, C. Y. *Proc. Natl. Acad. Sci. U.S.A.* **2006**, *103*, 5273.
(32) Zhang, B.; Zhang, Y.; White, H. S. *Anal. Chem.* **2004**, *76*, 6229.
(33) Zhang, B.; Galusha, J.; Shiozawa, P. G.; Wang, G.; Bergren, A. J.; Jones, R. M.; White, R. J.; Ervin, E. N.; Cauley, C. C.; White, H. S. *Anal. Chem.* **2007**, *79*, 4778.
(34) White, R. J.; Ervin, E. N.; Yang, Y.; Chen, X.; Daniel, S.; Cremer, P. S.; White, H. S. *J. Am. Chem. Soc.* **2007**, *129*, 11766.
(35) Butler, T. Z.; Gundlach, J. H.; Troll, M. *Biophys. J.* **2007**, *93*, 3229.
(36) Howorka, S.; Bayley, H. *Biophys. J.* **2002**, *83*, 3202.
(37) Muthukumar, M. *J. Chem. Phys.* **2003**, *118*, 5174.
(38) Tian, P.; Smith, G. D. *J. Chem. Phys.* **2003**, *119*, 11475.
(39) Han, J.; Craighead, H. G. *Anal. Chem.* **2002**, *74*, 394.
(40) Henrickson, S. E.; Misakian, M.; Robertson, B.; Kasianowicz, J. J. *Phys. Rev. Lett.* **2000**, *85*, 3057.
(41) Hille, B. *Ionic Channel of Excitable Membrane*, 2nd ed.; Sinauer Associates: Sunderland, MA, 1992.
(42) Meller, A.; Branton, D. *Electrophoresis* **2002**, *23*, 2583.
(43) Ma, S. K. *Statistical Physics*; World Scientific: Philadelphia, PA, 1985.
(44) De Gennes, P. D. *Adv. Polym. Sci.* **1999**, *138*, 91.
(45) Mathe, J.; Aksimentiev, A.; Nelson, D. R.; Schulten, K.; Meller, A. *Proc. Natl. Acad. Sci. U.S.A.* **2005**, *102*, 12377.